

Ferroelectric phase transition in $\text{Ba}_5\text{RTi}_3\text{Nb}_7\text{O}_{30}$ [R = Nd, Eu, Gd] ceramics

R N P CHOUDHARY*, S R SHANNIGRAHI and A K SINGH

Department of Physics, Indian Institute of Technology, Kharagpur 721 302, India

MS received 10 August 1998; revised 2 August 1999

Abstract. Polycrystalline samples of $\text{Ba}_5\text{RTi}_3\text{Nb}_7\text{O}_{30}$ [R = Nd, Eu, Gd], were prepared using high-temperature solid-state reaction technique. Preliminary X-ray structural analysis of the compounds shows the formation of single phase compounds (orthorhombic crystal system) at room temperature. Detailed studies of dielectric properties (ϵ , $\tan \delta$, σ) as a function of frequency (400 Hz to 10 kHz) and temperature (30° to 380°C) show that these compounds exhibit diffuse ferroelectric phase transition.

Keywords. Polycrystalline; ferroelectric; tungsten-bronze structure; dielectric constant; electrical conduction.

1. Introduction

Since the discovery of ferroelectricity in BaTiO_3 (Wul and Goldman 1945), a large number of simple or complex ferroelectric oxides of perovskite of a general formula ABO_3 (A = mono or divalent, B = tri to hexavalent ions) (Subbarao 1973) and tungsten-bronze (TB)-type structures (Magneli 1949) have extensively been studied in search of materials for device applications. Some niobates with TB-type structure such as barium niobates (BNN) (Rubin *et al* 1967), potassium niobates (KLN) (Uitert *et al* 1967), etc are considered to be interesting and attractive because of their wide industrial applications. It has been found that this family possesses many interesting physical properties such as electrooptic (Nenzo *et al* 1967), elasto-optic, pyroelectric (Glass 1969), acousto-optic (Ventiurini *et al* 1969), nonlinear (Abraham *et al* 1971), etc. The TB-type structure consists of a complex array of distorted BO_6 octahedral sharing corners in such a way that three different types of interstices (A, B and C) are available for cation substitutions (Jamieson *et al* 1965). The general formula commonly used for this family is $(\text{A}_1)_4(\text{A}_2)_2(\text{C})_4(\text{B}_1)_2(\text{B}_2)_8\text{O}_{30}$ in which a wide variety of substitution can be made for different applications. It has been found that this family has phase transition well above and well below the room temperature with sharp and/or diffuse-type (Mukherjee 1978). Though some studies have been reported on $\text{Ba}_2\text{Na}_3\text{RNb}_{10}\text{O}_{30}$ (R = La, Y, Gd, Eu and Dy) (Iwaski 1971), $\text{K}_2\text{LaNb}_5\text{O}_{15}$ (Ismailzade 1963), $\text{Ba}_{1/x}\text{R}_{2x/3}\text{Nb}_2\text{O}_6$ (Masuno 1964) and $\text{Ba}_4\text{NaNb}_{10}\text{O}_{30}$ (Subbarao 1987) earlier, no work has so far been reported on $\text{Ba}_5\text{RTi}_3\text{Nb}_7\text{O}_{30}$ (R = rare-earth ions)

family. Further, it has also been observed that the size of the substituted ions has significant effect on the disorderness of the structure (Lines and Glass 1977) and diffuseness of the phase transition in this family. In view of importance of the materials and non-availability of the ferroelectric data, we have carried out structural and dielectric properties studies of $\text{A}_5\text{RB}_3\text{Nb}_7\text{O}_{30}$ [R = Dy, Sm, Nd, Eu, Gd, La, Y; A = Ba, Sr; B = Zr, Ti]. In this paper we report our work on $\text{Ba}_5\text{RTi}_3\text{Nb}_7\text{O}_{30}$ (R = Nd, Eu, Gd).

2. Experimental

Polycrystalline samples of $\text{Ba}_5\text{NdTi}_3\text{Nb}_7\text{O}_{30}$, $\text{Ba}_5\text{EuTi}_3\text{Nb}_7\text{O}_{30}$ and $\text{Ba}_5\text{GdTi}_3\text{Nb}_7\text{O}_{30}$ (abbreviated as A, B and C compounds), were prepared from high-purity BaCO_3 (99.9%, M/s BDH), Nd_2O_3 , Eu_2O_3 and Gd_2O_3 (99.9%, M/s Indian rare-earth Limited), TiO_2 and Nb_2O_5 (99.9%, M/s S.D.fine-chem.) using high-temperature solid-state reaction technique. These ingredients taken in stoichiometry were mixed thoroughly in an agate mortar for 2 h and dried by slow-evaporation for 48 h and kept at 200°C for 24 h to dry the powders. The dried powders of the compounds were then calcined at 1000°C in a platinum crucible for 24 h. The process of mixing and calcination was repeated twice to get the homogeneous (400 mesh) powders. Finally, cylindrical pellets of the materials (diameter 10 mm and thickness = 1–2 mm) were prepared using hydraulic press at the pressure of $6 \times 10^7 \text{ N/m}^2$. These pellets were then sintered at 1250°C for 24 h to obtain high density (~95% of the theoretical value) ceramic samples. The quality and formation of the compounds were checked using X-ray diffraction technique (XRD). Room temperature (30°C) and X-ray diffractograms of the above A, B and C compounds were

*Author for correspondence

recorded using Phillips (Netherlands) powder diffractometer with $\text{CuK}\alpha$ radiation ($\lambda = 0.15418 \text{ nm}$) in a wide range of 2θ ($20^\circ \leq 2\theta \leq 65^\circ$) at a scanning rate of $2^\circ/\text{min}$. To measure the electrical properties; dielectric constant (ϵ), tangent loss ($\tan \delta$) and electrical conductivity (σ) of these compounds, both the faces of the pellet samples were electroded with silver paint and samples were kept at 100°C for 24 h to remove moisture. Measurements of capacitance and dissipation factor were carried out by GR 1620 capacitance measuring assembly, both as a function of frequency ($400\text{--}10^4 \text{ Hz}$) and temperature ($30^\circ\text{--}380^\circ\text{C}$) in the heating and cooling mode ($1^\circ/\text{min}$) in dry air atmosphere. From the capacitance measurements, the dielectric permittivity was determined whereas the dissipation factor was used to calculate the tangent loss at different frequencies and temperatures. Measurements were repeated in the same conditions as above after 6 months and a small variation (5%) was found, indicating the stability of the compounds. The room temperature dc electrical resistivity (σ_{dc}) of both the samples was measured both as a function of biasing electric field ($30\text{--}100 \text{ V/cm}$) and temperature at a particular field. The Keithley 617 programmable electrometer, laboratory fabricated 2-terminal sample holder and furnace were used for the experiment. Cromel-alumel thermocouple was used to measure temperature.

3. Results and discussion

The sharp and single XRD peaks of all the samples suggest the formation of single-phase compounds. All the XRD peaks were indexed in different crystal systems in different three configurations using their experimental (interplanar spacing) d -values in a standard computer program, Powdmult. Finally, unit cells of orthorhombic crystal system were selected on the basis of minimization of $\Sigma\Delta d = \Sigma(d_{\text{obs}} - d_{\text{cal}})$. The selected cell parameters were refined using least-squares method. These are: $a = 7.180$, $b = 5.059$, $c = 7.571 \text{ \AA}$ for the compound A; $a = 7.118$, $b = 7.414$, $c = 7.939 \text{ \AA}$ for the compound B; and $a = 7.8184$, $b = 5.157$, $c = 8.402 \text{ \AA}$ for the compound C (with estimated error = 0.001 \AA). Good agreement between calculated and observed interplanar spacings (d_{obs} and d_{cal}) was observed for all the three, A, B, C samples. It was not possible to determine the space group of the compounds with limited powder data. The particle size of the compounds was calculated from a few reflection peaks widely spread in 2θ range using Scherrer's equation,

$$P_{hkl} = \frac{k\lambda}{\beta_{1/2} \cos \theta_{hkl}},$$

where $k = 0.89$ and $\beta_{1/2}$ = half peak width. The average particle size was found to be 220 \AA , 250 \AA and 235 \AA for

A, B, C compounds, respectively, which are comparable to those of the other ferroelectrics prepared with the above method.

At room temperature, the variation of dielectric constant (ϵ) and loss tangent ($\tan \delta$) of the A, B, C compounds with frequency ($400\text{--}10^4 \text{ Hz}$) is shown in figure 1. ϵ decreases gradually with increase in frequency in the case of B and C containing compounds but it remains almost invariant for the A compound. Moreover, the variation of ϵ for B compound is very fast compared to that of the C compound and for the case of $\tan \delta$ we observed peaks for A and B but not for C. As expected, dielectric peak of the compounds does not coincide with that of loss. Figure 2 shows the variation of dielectric constant with temperature at two different frequencies, 10^3 Hz and 10^4 Hz . We observed that all the compounds have dielectric anomaly. For Eu containing compound (i.e. B), there is a large difference in the values of ϵ at low frequencies. There is an increase in ϵ beyond 310°C for Nd containing compound (i.e. A), which may be due to

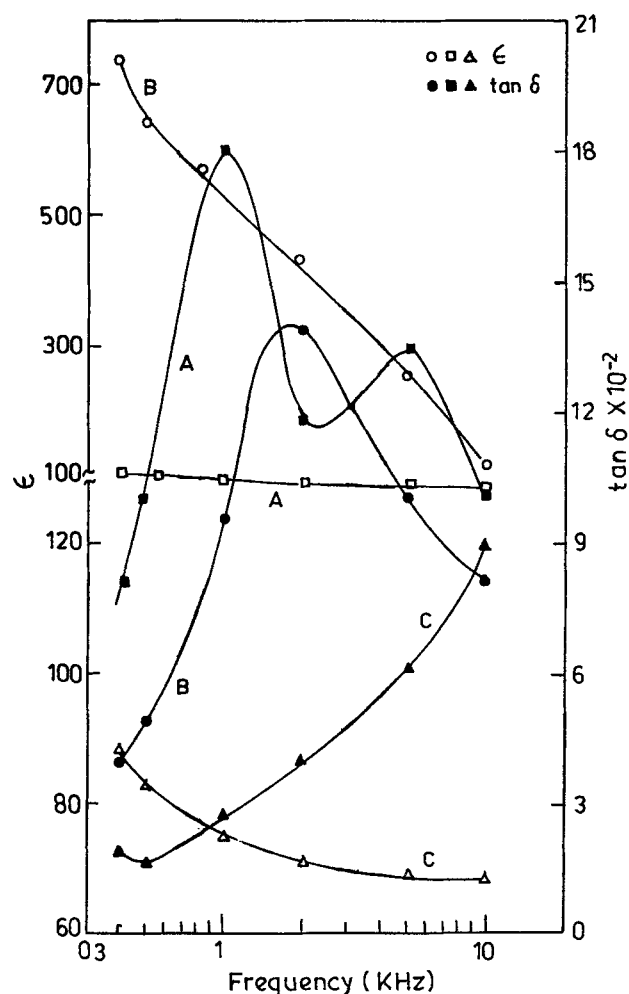


Figure 1. Variation of dielectric constant (ϵ) and loss ($\tan \delta$) of $\text{Ba}_5\text{NdTi}_3\text{Nb}_7\text{O}_{30}$ (A), $\text{Ba}_5\text{EuTi}_3\text{Nb}_7\text{O}_{30}$ (B), $\text{Ba}_5\text{GdTi}_3\text{Nb}_7\text{O}_{30}$ (C) with frequency at room temperature.

the presence of space charge polarization in high-temperature region. The region around the dielectric peak was found broadened in all three cases. The broadening of the dielectric peak may be considered due to the disorder in the arrangements of rare earth and other atoms leading to a microscopic heterogeneity in the composition, and thus a distribution of different local Curie points results. The structural disorder in the compounds arises due to the presence of number of voids and size of impurities. Dielectric constant (ϵ) and phase transition temperature at 10^3 Hz and 10^4 Hz frequencies are shown in table 1. Anomaly in $\tan \delta$ was observed in the case of A and B containing compounds (figure 3). At 10^4 Hz, C compound has also got a peak. The high value of loss tangent in each material is due to transport of ions at higher thermal energy. The degree of disorder or diffusivity (γ), in the A, B and C compounds was calculated using the expression (Pilgrim *et al* 1990),

$$\ln \left(\frac{1}{\epsilon} - \frac{1}{\epsilon_{\max}} \right) = \gamma \ln(T - T_c) + a,$$

where ϵ_{\max} is the maximum value of ϵ at T_c and γ the diffusivity of the broadening peak. The values of γ calculated from the slope of graphs (figure 4) were found to be 1.9 and 1.8 for A and C compounds which confirms

the diffuse phase transition in the materials. The ac dielectric conductivity (σ) and activation energy (E_a) of the compounds in the high-temperature region (i.e. in paraelectric phase) were calculated from the measured dielectric data and using the formula (Gurevich 1969),

$$\sigma = \epsilon \epsilon_0 \omega \tan \delta = \sigma_0 \exp(-E_a/K_B T),$$

where ϵ_0 is the vacuum dielectric, ω the angular frequency and K_B the Boltzmann constant. The plot of $\ln \sigma$ vs $10^3/T$ (figure 5) shows the change in slope exactly at the transition temperature of the materials as observed in dielectric studies. Such type of anomaly has been

Table 1. Comparison of some dielectric properties of $Ba_5RTi_3Nb_7O_{30}$ (R = Nd, Eu, Gd) at 1 kHz and 10 kHz.

Compound	Freq. (kHz)	ϵ_{\max}	ϵ_{RT}	T_c (°C)	ν	ρ (ohm-cm)
R = Nd	1	220	128	267	1.9	1.46×10^9
	10	212	126	269	1.9	
R = Eu	1	640	596	266	1.2	2.1×10^8
	10	166	110	268	1.2	
R = Gd	1	115	76	288	1.8	1.6×10^8
	10	88	64	289	1.8	

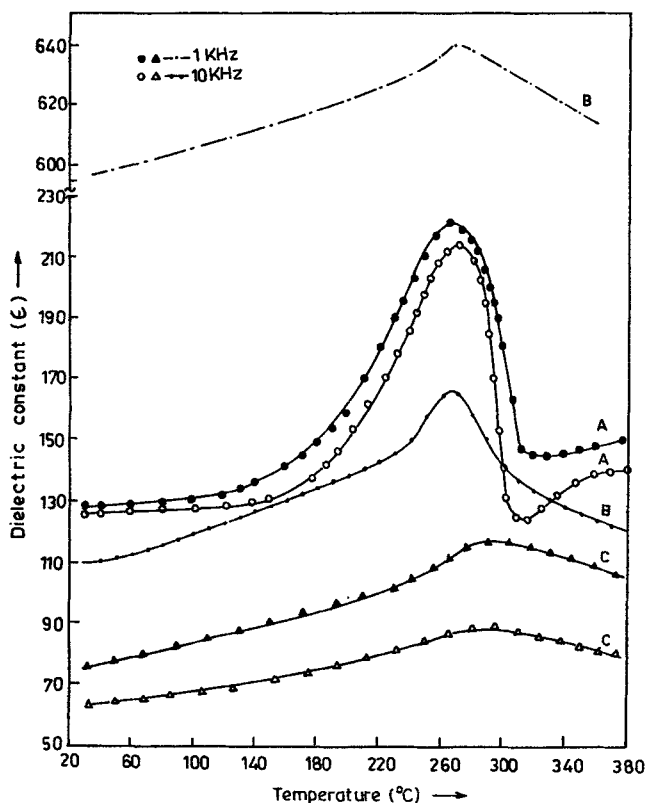


Figure 2. Variation of dielectric constant (ϵ) of $Ba_5NdTi_3Nb_7O_{30}$ (A), $Ba_5EuTi_3Nb_7O_{30}$ (B), $Ba_5GdTi_3Nb_7O_{30}$ (C) as a function of temperature at 10 kHz and 1 kHz.

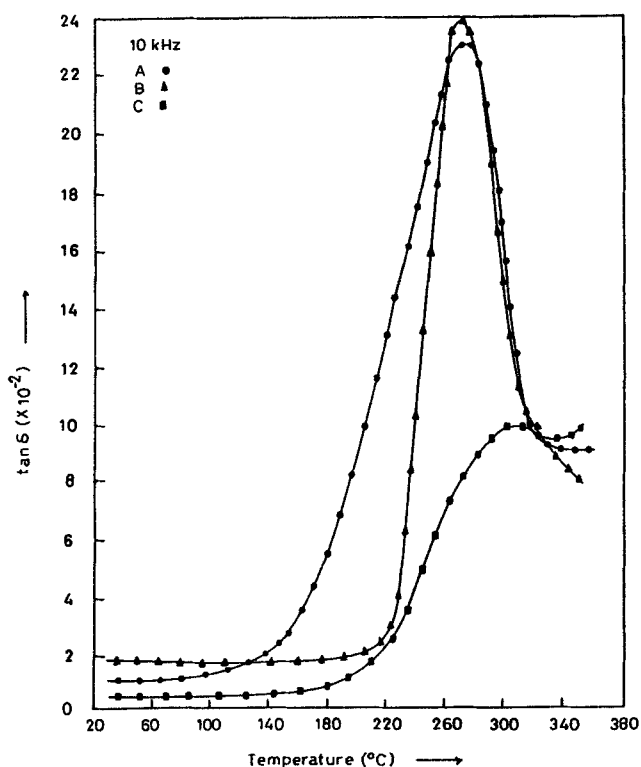


Figure 3. Variation of dielectric loss ($\tan \delta$) of $Ba_5NdTi_3Nb_7O_{30}$ (A), $Ba_5EuTi_3Nb_7O_{30}$ (B), $Ba_5GdTi_3Nb_7O_{30}$ (C) as a function of temperature at 10 kHz and 1 kHz.

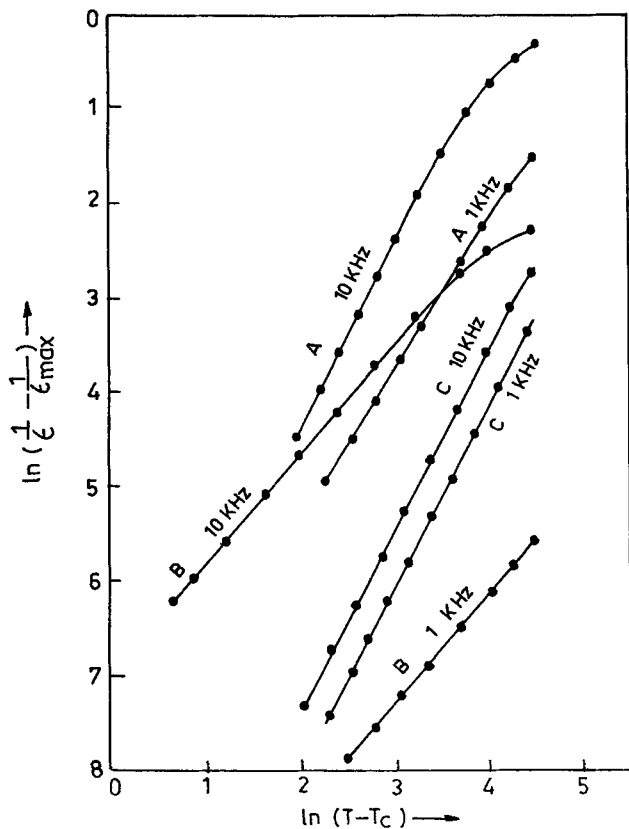


Figure 4. Variation of $\ln(1/\epsilon - 1/\epsilon_{max})$ of $Ba_5NdTi_3Nb_7O_{30}$ (A), $Ba_5EuTi_3Nb_7O_{30}$ (B), $Ba_5GdTi_3Nb_7O_{30}$ (C) with $\ln(T - T_c)$.

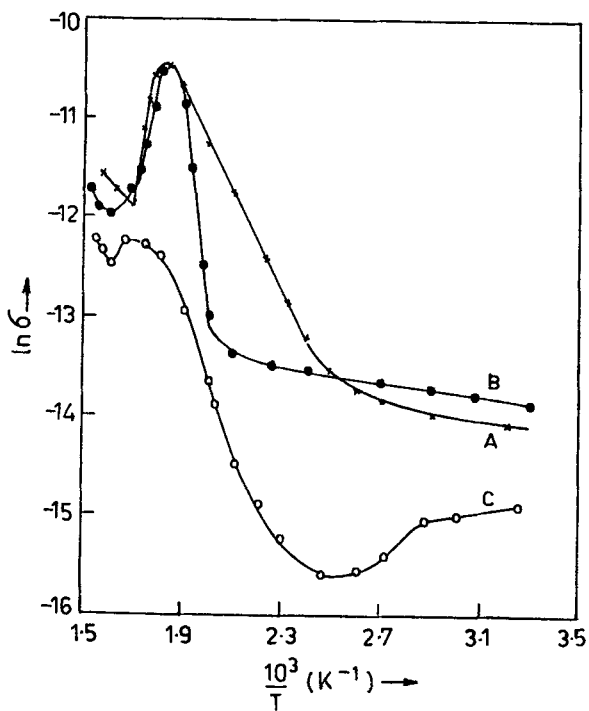


Figure 5. Variation of ac conductivity ($\ln \sigma$) of $Ba_5NdTi_3Nb_7O_{30}$ (A), $Ba_5EuTi_3Nb_7O_{30}$ (B), $Ba_5GdTi_3Nb_7O_{30}$ (C) with inverse of absolute temperature ($10^3/T$).

observed in many other ferroelectric ceramics. This is due to the difference in activation energy in the paraelectric and ferroelectric phases. In the above materials, we did not get an exact transition temperature but a transition region that could be explained by the coexistence of the paraelectric and ferroelectric phase over some temperature region. But in the case of C compound we saw some peculiarity in the temperature range $30^\circ - 127^\circ C$. The difference in the activation energy between the paraelectric and ferroelectric phases is due to the grain boundary effect. However, this has not been confirmed by

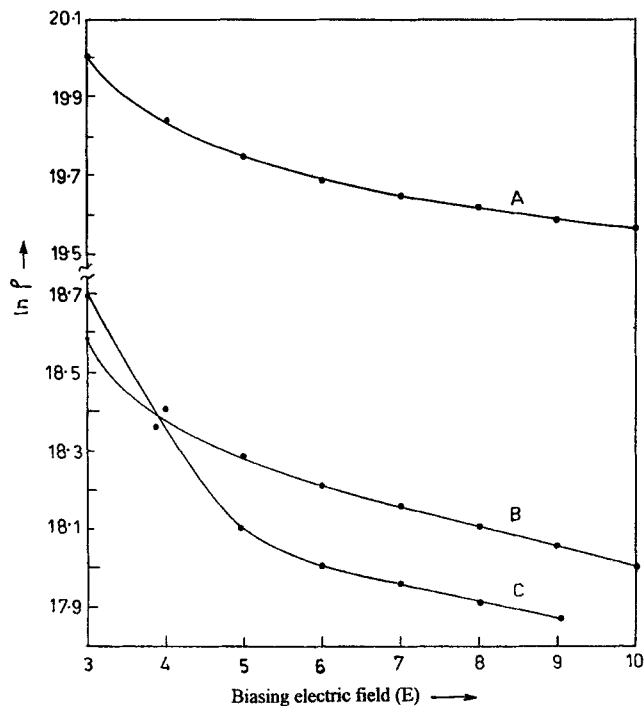


Figure 6. Variation of dc resistivity ($\ln \rho$) of $Ba_5NdTi_3Nb_7O_{30}$ (A), $Ba_5EuTi_3Nb_7O_{30}$ (B), $Ba_5GdTi_3Nb_7O_{30}$ (C) with a biasing electric field (V) at room temperature.

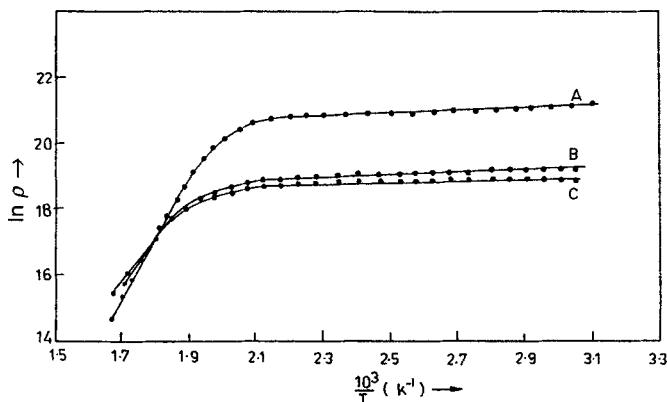


Figure 7. Variation of dc resistivity ($\ln \rho$) of $Ba_5NdTi_3Nb_7O_{30}$ (A), $Ba_5EuTi_3Nb_7O_{30}$ (B), $Ba_5GdTi_3Nb_7O_{30}$ (C) with inverse of absolute temperature ($10^3/T$).

our macroscopic studies. Activation energy of all the materials (A, B, C) in paraelectric phase at frequency 10^4 Hz is tabulated in table 1. Figure 6 shows the variation of $\ln \rho$ with applied voltage. We observed the decrease in $\ln \rho$ by increasing field, which shows alignment of dipoles with the field, which is observed in some ferroelectrics of perovskite family (Singh *et al* 1992a, b). Figure 7 shows the variation of $\ln \rho$ with $10^3/T$. Similar variation has been found in many ferroelectric ceramics (Shannigrahi *et al* 1998).

4. Conclusion

There is no change in the basic structure of $Ba_5RTi_3Nb_7O_{30}$ for substitution of different rare earth elements. One can see a very significant change in dielectric permittivity of materials even if they (Nd, Eu, Gd) belong to the same periodic group and are very close to each other. Their transition temperatures are almost equal. It is also observed that all transitions are of diffuse-type. The higher value of E_a for B is an indication that it is not a good semiconductor, whereas other two materials are good semiconductors.

References

- Abraham S C, Jamieson P B and Bernstein J L 1971 *J. Chem. Phys. Lett.* **54** 2355
 Glass A M 1969 *J. Appl. Phys.* **40** 4699
 Gurevich V M 1971 *Electric conductivity of ferroelectrics* (Jerusalem: Israel Program for Scientific Translations)
 Ismailzade I G 1963 *Sov. Phys. Cryst.* **8** 351
 Iwaski H 1971 *Mater. Res. Bull.* **6** 251
 Jamieson P B, Abraham S C and Bernstein J L 1965 *J. Chem. Phys.* **48** 5048
 Lines M E and Glass A M 1977 *Principles and applications of ferroelectric and related materials* (London: Oxford University Press)
 Magneli A 1949 *Ark. Chem.* **1** 213
 Masuno K V 1964 *J. Phys. Soc. Japan* **19** 323
 Mukherjee J L 1978 *J. Solid State Chem.* **24** 163
 Nenzo P V, Spencer E G and Balmann A A 1967 *J. Appl. Phys. Lett.* **11** 23
 Pilgrim S M, Sutherland A E and Winzer S R 1990 *J. Am. Ceram. Soc.* **73** 3122
 Rubin J J, Van Uitert L B and Levinstein H J 1967 *J. Cryst. Growth* **1** 315
 Shannigrahi S R, Choudhary R N P, Kumar Atul and Acharya H N 1998 *J. Phys. Chem. Solids* **59** 737
 Singh K S, Sati R and Choudhary R N P 1992a *J. Mater. Sci. Lett.* **11** 788
 Singh K S, Sati R and Choudhary R N P 1992b *Pramana - J. Phys.* **38** 161
 Subbarao E C 1973 *Ferroelectrics* **5** 267
 Subbarao P S V 1987 *J. Mater. Sci. Lett.* **6** 299
 Uitert L B, Singh S, Levinstein H J, Gensic J F and Bonner W A 1967 *Appl. Phys. Lett.* **11** 161
 Venturini E L, Spencer E G and Ballman A A 1969 *J. Appl. Phys.* **40** 1622
 Wul B K and Goldman L M 1945 *C. R. Acad. Sci. (USSR)* **46** 133